

SYNTHESIS OF CeO₂-COATED TiO₂ MICROPARTICLES AND PHOTOCATALYTIC DEGRADATION OF METHYLENE BLUE

Ali İmran VAİZOĞULLAR, Ahmet BALCI, Mustafa Tamer UZUN, Mehmet UĞURLU

Muğla Sıtkı Koçman University, Faculty of Science, Department of Chemistry, 48000-
MUĞLA

Abstract: TiO₂ nanoparticle layed sol-gel method that was coated with CeO₂ by means of chemical precipitation technique. X-ray diffraction (XRD), infrared (IR) spectra, scanning electron microscopy (SEM) of X-ray (EDAX), and transmission electron microscopy (TEM) were used to characterize the CeO₂-coated TiO₂ particles. XRD patterns showed that the core area of the core shell particles was amorphous SiO₂, and the shell area was fluorite-structured CeO₂. IR results indicated that the coating of the TiO₂ nanoparticle with CeO₂ evidently induced the presence of new bands at 1711, 1620, 1554, 1192 ve 1040 cm⁻¹, belonging to Ce-O-Ti bands. SEM and TEM analysis showed that CeO₂-coated TiO₂ microparticles showed a spherical morphology with the diameter about 0,5-1 µm and a uniform particle size. Photoactivity of TiO₂ and TiO₂/CeO₂ core shell particles degradation for Methylene Blue (MB) and Methylene Orange (MO) was found that %41 and %34 respectively for TiO₂/CeO₂ core shell particles. The photoactivity of TiO₂ was decreased after coated with CeO₂ with in 90 min

1. Introduction

In these days, there has been a great interest in the preparation of core-shell structured materials such as sol-gel [1,2], microemulsion [3-4], thermal reduction [5], and hot injection method [6]. Although the microemulsion method has the advantage of the precise control of particle size and morphology at mild temperatures and pressures [7], sol gel method has a wide of applications. Ceria (CeO₂) is a cubic fluorite-type structured ceramic material that does not show any known crystallographic change from room temperature up to its melting point (2700°C) [8-9]. Cerium oxide (CeO₂) is a versatile rare-earth oxide material that has frequently been used as an industrial catalyst in processes such as catalytic cracking, methanol dissociation, water-gas shift reaction and automotive emission control, due to its characteristic oxygen storage/release property [10]. As well as it uses in many applications, such as UV absorbents and filters [11-12], electrolytes in the fuel cell technology [13-14],

water-gas shift catalysts [15-16], polishers for chemical mechanical planarization (CMP) [17-18], etc. Most of the applications require the use of non-agglomerated nanoparticles, as aggregated nanoparticles lead to inhomogeneous mixing and poor sinterability [19]. Catalytic properties of CeO_2 have been attributed to the formation of Ce^{+3} defect sites and subsequent oxygen vacancies. CeO_2 is n-type semiconductor and has band gap energy that 2,7-3,4 eV, CeO_2 is generally known as inactive material. Researcher worked that about the electron localization of CeO_2 with precise observation of high-resolution scanning tunneling microscopy reveals that the defects of CeO_2 are difficult to move. In this study, the preparation of silica–ceria, core–shell microparticles was synthesised using sol gel method and their photocatalytic activity in methylene blue.

2. Materials And Methods

2.1. Chemicals

Chemicals used in the synthesis were tetraethylorthosilicate (TEOS), cerium nitrate hexahydrate ($\text{Ce}(\text{NO}_3)_3 \cdot 6\text{H}_2\text{O}$), Ethanol ($\text{C}_2\text{H}_5\text{OH}$), NaOH solution (0,01M) and CTAB.

2.2. Preperation of materials

2.2.1. Preparation of TiO_2

The TiO_2 core was prepared by the sol–gel method and hydrolysis and polycondensation of TBT. 10 ml TBT and 25 ml absolute ethanol were mixed into 50 ml deionized water. Later, the mixed solution was stirred for 4 h after that solutions were separated by centrifugation, the particles washed several times with deionized water and ethanol before drying at 80 °C for 4 h. The latest final TiO_2 microparticle was obtained by calcining the above powder at 600 °C for 3 h.

2.2.2. $\text{TiO}_2/\text{CeO}_2$ core shell particles

CeO_2 -coated TiO_2 microparticle was prepared by chemical precipitation method. TiO_2 microparticle prepared above was used as core for the coating experiment. First, 1.0 g TiO_2 cores and 1.5 g $\text{Ce}(\text{NO}_3)_3 \cdot 6\text{H}_2\text{O}$ were dissolved into 100 ml water that containing 0.2 g CTAB. The solution was dispersed for 30 min after its pH value was adjusted to about 10 by using 0.01 mol l^{-1} NaOH solution. Mixed solution was stirred for 4 h at aged for 2 h. The latest particles was collected by filtration, washing with deionized water for several times to remove contaminants, followed by drying overnight at 80 °C in vacuum and calcination at 400 °C for 3h.

2.3. Characterization

The crystalline phase and the component of the sample were examined by XRD(RigakuDmax 350) using copperK_α radiation ($\lambda = 0.154056$ nm). The IR spectrum analysis of precursor was carried out employing IR measurement system Thermo-Scientific, (Nicolet IS10-ATR). The microstructure and shape of the particle were investigated by SEM (JEOL JSM-7600F) and TEM (JEOL JEM 2100F HRTEM). The element was determined using (JEOL JSM-7600F) EDAX analyser with SEM measurement. XRD analysis were examined (RIKAGU-SMART LAB) measurement.

3. Results and discussion

3.1. XRD analysis of CeO₂ and CeO₂-coated SiO₂ nanoparticle

XRD patterns of the as-prepared CeO₂ (a) and TiO₂ (b) and CeO₂-coated TiO₂ (c) microparticle are shown in Fig. 1 and 2. In both particles we observed characteristic CeO₂ peaks that was corresponding to the four strongest peaks of fluorite-structured CeO₂ (28.43, 32.92, 47.38, 56.27) diffractograms of the TiO₂/CeO₂ core shell microparticle (Fig. 1). It means that the shell area of the core shell particles is CeO₂.

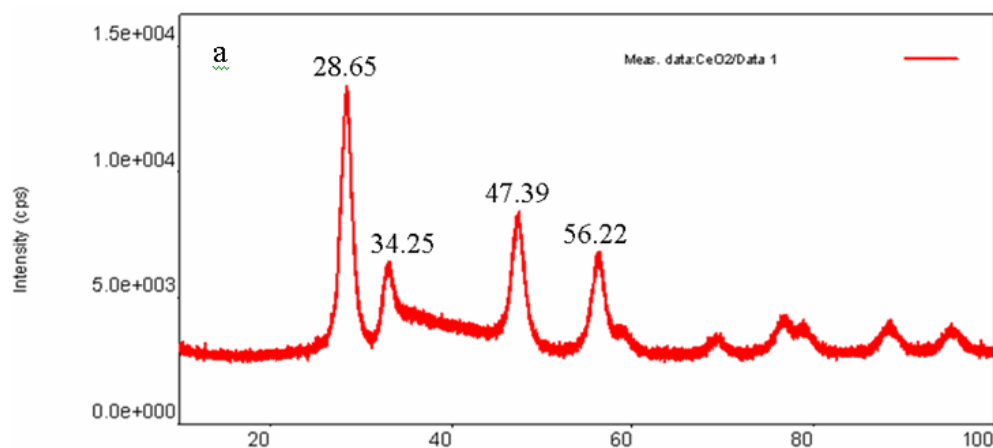


Fig. 1. XRD patterns of CeO₂ microparticles

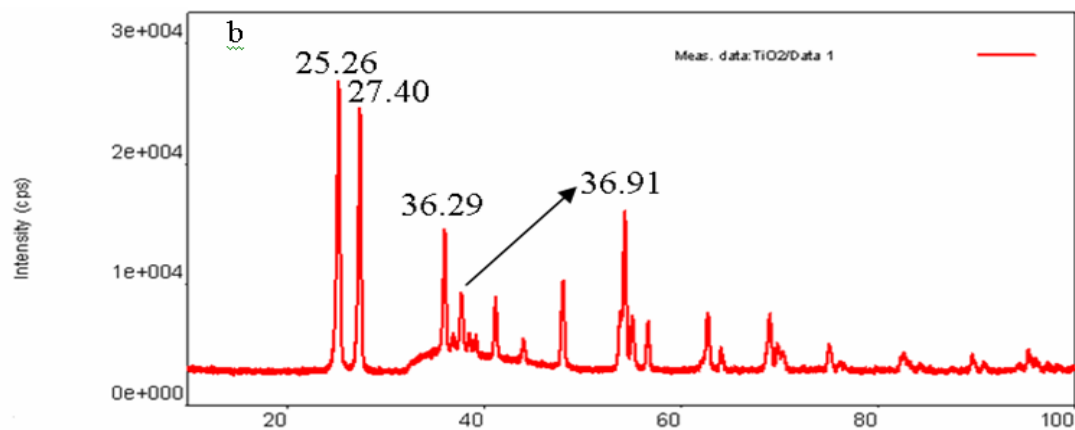


Fig. 2. XRD patterns of TiO₂ microparticles

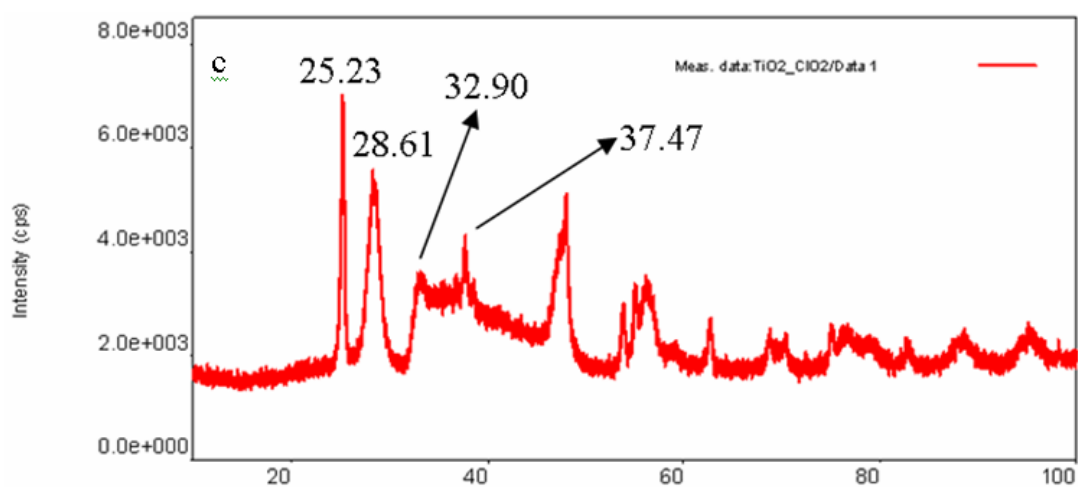


Fig. 3. XRD patterns of CeO₂-coated TiO₂ microparticle

We observed peak corresponding to the characteristic of an amorphous TiO₂ 24.26°, 27.40°, 36.29° ve 36.91° (Fig. 1). Figure 3 shows us that two different spectrum respectively. In one of these belonging to TiO₂ and other one is CeO₂ (25,23° and 28,61°). It means that TiO₂/CeO₂ particles were synthesised completely which is confirmed with the observation of SEM and TEM images.

3.2. FTIR analysis

FTIR measurement was measurement for TiO₂ microparticle, and TiO₂/ CeO₂ core shell particle as shown in Fig.4 and 5. O-H bands from water is detected with around 3430 cm⁻¹, corresponding to O–H stretching frequency, and (Fig. 4). [Ti(OH)₂²⁻] stretching at between 1640 cm⁻¹ and 1450 cm⁻¹. Figure 5 shows that 1620 cm⁻¹ is belonging to Ti-O-Ti stretching. 2255 cm⁻¹ is belonging to TiOH₂²⁻. Comparing the spectra of TiO₂ microparticle and the

TiO₂/CeO₂ core shell microparticle the band at 1711, 1620, 1554, 1192 ve 1040 cm⁻¹ is belonging to TiO₂/CeO₂ microparticles.

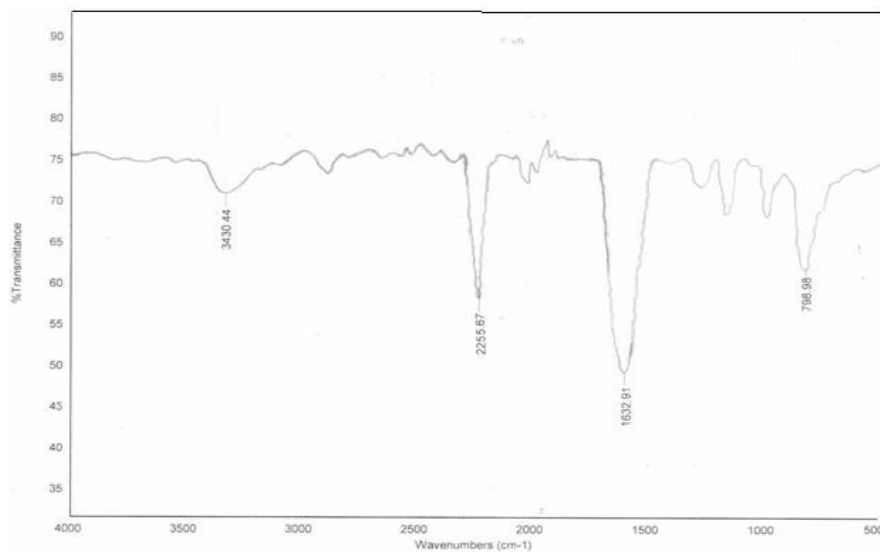


Fig. 3. IR spectra of TiO₂ microparticle

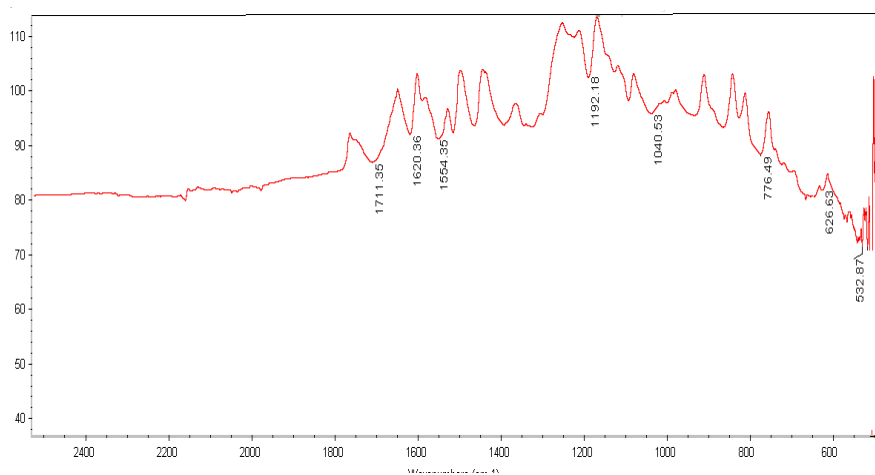


Fig. 4. IR spectra of TiO₂/ CeO₂ core shell microparticle.

3.1.4. SEM and EDAX

SEM analysis gives information about size and shape of particles. Fig. 6 and 7 shown that TiO₂ particles and of the TiO₂/CeO₂ core shell particles in the SEM images. Monodisperse and very uniform spheres can be clearly observed (Fig. 6). Particle size of the TiO₂/CeO₂ core shell particles, is approximately 500-1000 nm (Fig. 7). EDAX carried out on TiO₂/CeO₂ core shell particle indicated qualitatively the presence of CeO₂ (Fig. 7).

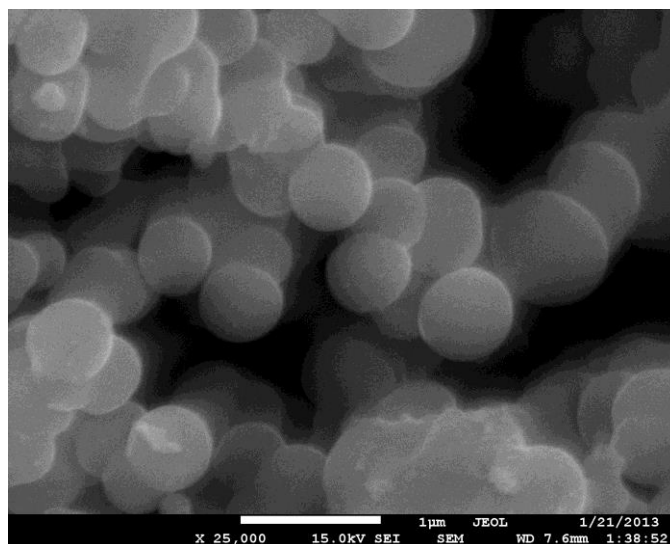
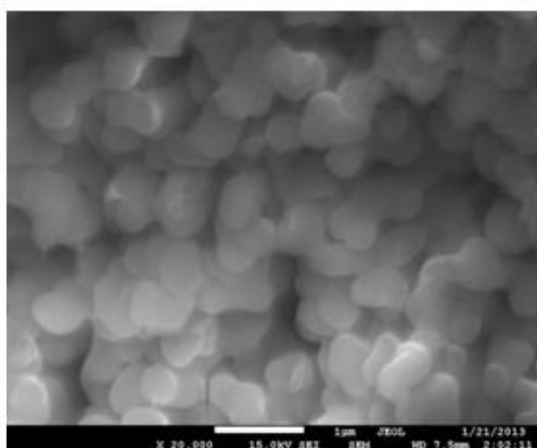
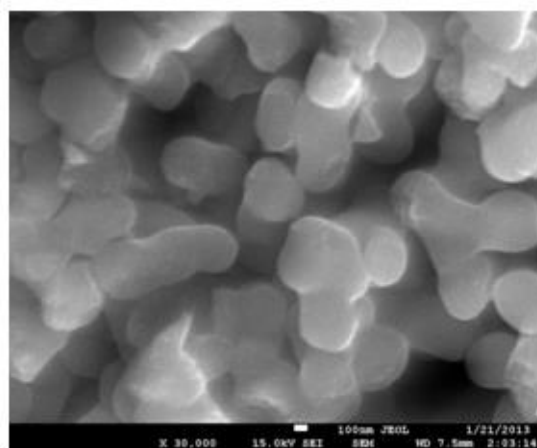


Fig. 5. SEM images of TiO₂ particles



(a)



(b)

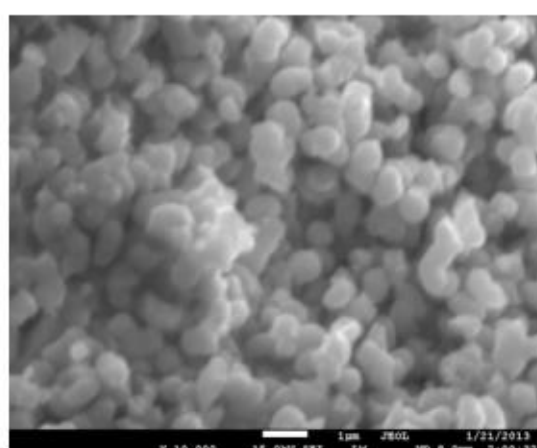
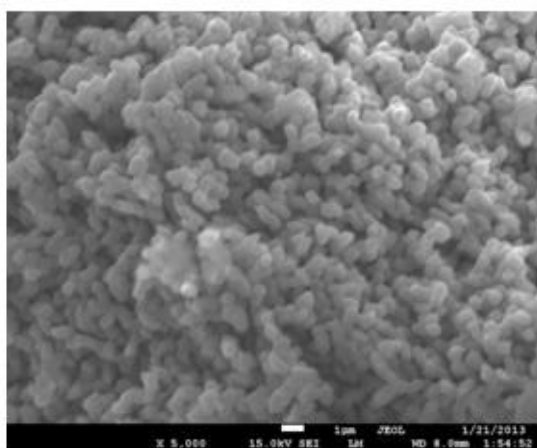


Fig. 6. SEM images of TiO₂/CeO₂ core shell particles

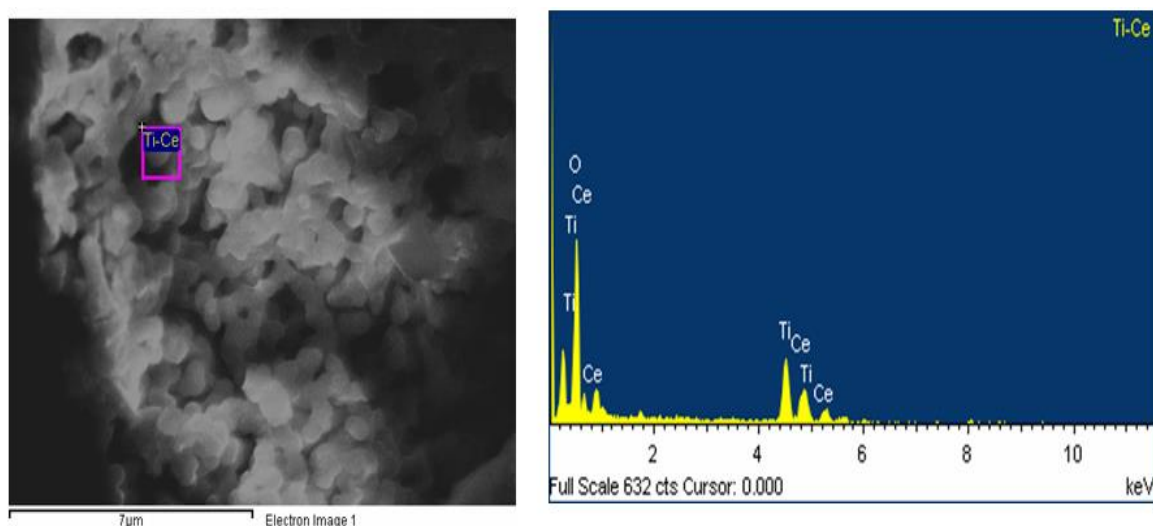


Fig. 7. EDAX analysis of $\text{TiO}_2/\text{CeO}_2$ core shell particles

3.4. TEM analysis

Fig. 9 show TEM images of the $\text{TiO}_2/\text{CeO}_2$ core shell particles. After coating, particle size of the microparticles increases, and a characteristic stage of CeO_2 with a lighter opposition and shagginess can be clearly observed, which shows the presence of $\text{TiO}_2/\text{CeO}_2$ core shell particles.

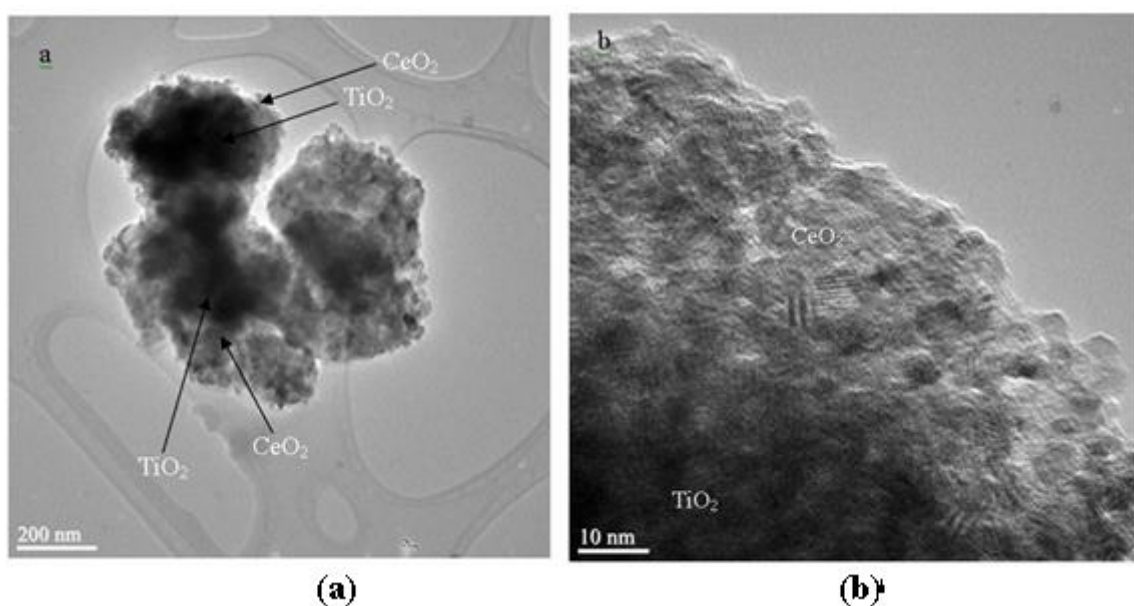


Fig. 9. TEM analysis of $\text{TiO}_2/\text{CeO}_2$ core shell particles

3.5. Photocatalytic Activity in Methylene Blue

In this study, we investigated that degradation of MO and MB for TiO_2 particles and $\text{TiO}_2/\text{CeO}_2$ particles under UV light. Because CeO_2 is not photoactivity materials. Therefore we researched it, after coated TiO_2 layer what is shown activity. The photoactivity of TiO_2 particles are % 34 MO and % 41 MB respectively. But the photoactivity of $\text{TiO}_2/\text{CeO}_2$

particles is %6 MO and %46 MB. It can be explained that this surface of $\text{TiO}_2/\text{CeO}_2$ particles are negatively charge (Figure 9-10).

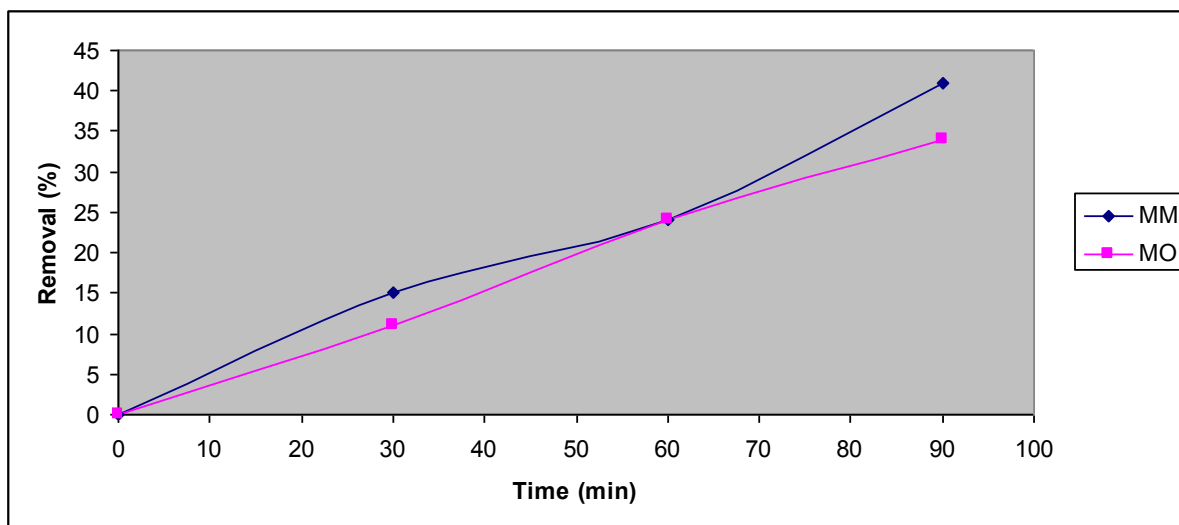


Fig. 9. Removal of MO and MB with TiO_2 particles in UV

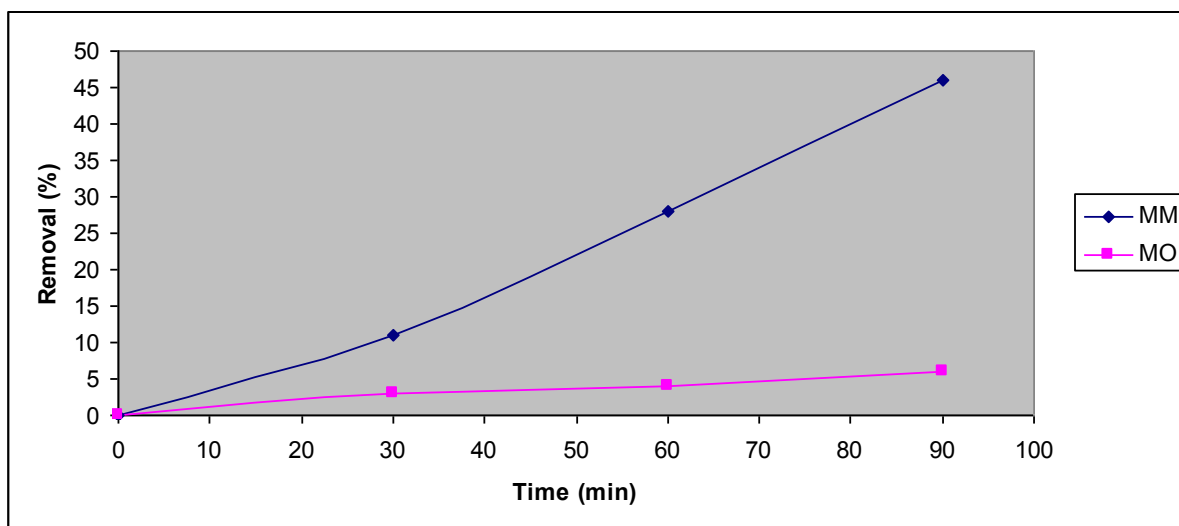


Fig.10. Removal of MO and MB with $\text{TiO}_2/\text{CeO}_2$ core shell particles under UV

3.6. Conclusion

In this study, the coating of CeO_2 on the TiO_2 particle surface was performed employing precipitation method. XRD study showed that the core area of the composite particle is amorphous TiO_2 , and the shell area is fluorite-structured CeO_2 . IR spectra showed that the coating of the TiO_2 particle with CeO_2 evidently gives at 1711, 1620, 1554, 1192 ve 1040 cm^{-1} is belonging to $\text{TiO}_2/\text{CeO}_2$ microparticles. SEM and TEM photos revealed that CeO_2 -coated TiO_2 particle possess uniform particle size about 500-600 nm in spherical shape and we showed CeO_2 particles was not contributed on TiO_2 surface homogenously.

References

- [1] H. Wang, M. Yu, C.K. Lin, J. Lin, *J. Colloid Interface Sci.* 300 (2006) 176.
- [2] Bin Li, Xi Wei, Wei Pan, *J. Power Sources* 193 (2009) 598.
- [3] L.M. Liz-Marzán, M. Giersig, P. Mulvaney, *Langmuir* 12 (1996) 4329.
- [4] D. Chen, J. Li, C. Shi, X. Du, N. Zhao, J. Sheng, S. Liu. *Chem. Mater.* 19 (2007) 3399.
- [5] X.D. He, X.W. Ge, M.Z. Wang, Z.C. Zhang, *J. Colloid Interface Sci.* 299 (2006) 791.
- [6] M. Ocana, M. Adres-Verges, R. Pozas, C.J. Serna, *J. Colloid Interface Sci.* 294 (2006) 355.
- [7] M.R. Kim, J.H. Chung, M. Lee, S. Lee, J.-J. Jang, *J. Colloid Interface Sci.* 350 (2010) 5.
- [8] R.P. Bagwe, K.C. Khilar, *Langmuir* 16 (2000) 905.
- [9] Corradi AB, Bondioli F, Ferrari AM, Manfredini T (2006). Synthesis and characterization of nanosized ceria powders by microwave–hydrothermal method. *Mater. Res. Bull.*, 41: 38–44.
- [10] Li J, Ikegami T, Wang Y, Mori T. Nanocrystalline $Ce_{1-x}Y_xO_{2-x/2}$ ($0 \leq x \leq 0.35$) Oxides via Carbonate Precipitation: Synthesis and Characterization. *J. Solid State Chem.*, (2002) 168: 52–59.
- [11] Sang-Ho Chung a, Dae-Won Lee b, Min-Sung Kim a, Kwan-Young Lee a, The synthesis of silica and silica–ceria, core–shell nanoparticles in a water-in-oil (W/O) microemulsion composed of heptane and water with the binary surfactants AOT and NP-5, *J. of Colloid and Interface Sci.* 355 (2011) 70–75
- [12] Cheviré F, Munoz F, Baker CF, Tessier F, Larcher O, Boujday S, Colbeau-Justin C, Marchand R (2006). UV absorption properties of ceria-modified compositions within the fluorite-type solid solution CeO_2 – Y_6WO_{12} . *J. Solid State Chem.*, 179: 3184–3190.
- [13] Souza ECC, Brito HF, Muccillo ENS (2010). Optical and electrical characterization of samaria-doped ceria. *J. Alloys Compd.*, 491: 460–464.
- [14] Matovic, B., Boskovic, S., Logar, M., Radovic, M., Dohcevic-Mitrovic, Z., Popovic, Z.V., Aldinger F. (2010). Synthesis and characterization of the nanometric Pr-doped ceria, *J. Alloys Compd.*, 505: 235–238.
- [15] Lapa, C.M., de Souza, D.P.F., Figueiredo, F.M.L., Marques, F.M.B. (2010). Two-step sintering ceria-based electrolytes, *Int. J. Hydrogen Energy*, 35: 2737–2741.
- [16] Gorte, R.J., Zhao, S. (2005) Studies of the water-gas-shift reaction with ceria-supported precious metals, *Catal. Today*, 104: 18–24.
- [17] Zhou XD, Huebner D, Anderson HU (2002). Size-induced lattice relaxation in CeO_2 nanoparticles. *Appl. Phys. Lett.*, 80: 3814–3816.
- [18] Xin J, Cai W, Tichy JA. A fundamental model proposed for material removal in chemical–mechanical polishing. *Wear*, (2010) 268: 837–844.
- [19] Jalilpour, M., and Fathalilou, M. Effect of aging time and calcination temperature on the cerium oxide nanoparticles synthesis via reverse co-precipitation method. *Int. J. of Phy. Sci.* (2012). 7(6), 944.
- [20] Li J, Ikegami T, Wang Y, Mori T (2002). Nanocrystalline $Ce_{1-x}Y_xO_{2-x/2}$ ($0 \leq x \leq 0.35$) Oxides via Carbonate Precipitation: Synthesis and Characterization. *J. Solid State Chem.*, (2002) 168: 52–59.
- [21] J.W. Raebiger, J.L. Manson, R.D. Sommer, U. Geiser, A.L. Rheingold, J.S. Miller, *Inorg. Chem.* 40 (2001) 2578.
- [22] N.J. Babu, A. Nangia, *Cryst. Growth Des.* 6 (2006) 1753;
- [25] Orel Z.C, Orel B. *Phys Status Solid B.* (1994) 186:33.
- [26] Esch, F., Fabris, S., Zhou, L., Montini, T., Africh, C., Fornasiero, P. Electron Localization determines defect formation on ceria substrates. *Sci.* (2005) 309:752.

- [27] Xiaolan Song, X., Nan Jiang, N., Yukun Li, Y., Dayu Xu, D., Guanzhou Qiu, G. Synthesis of CeO₂-coated SiO₂ nanoparticle and dispersion stability of its suspension, *Mat. Chem. and Phy.* 110 (2008) 128–135
- [28] Lin, Y., Xiaoming, Z. (2008) Preparation of highly dispersed CeO₂/TiO₂ core-shell nanoparticles. *Mat. Let.* (2008) 62: 3764.
- [29] Yue Lin , Zhang Xiaoming, Preparation of highly dispersed CeO₂/TiO₂ core-shell nanoparticles, *Materials Letters* 62 (2008) 3764–3766
- [30] Fu, X., Clark, L.A., Yang, Q., Anderson, M.A. (1996) Enhanced photocatalytic performance of titania-based binary metal oxides TiO₂/SiO₂ and TiO₂/ZrO₂, *Environ. Sci. Technol.*, 30: 647–653.
- [31] Konstantinou, I.K., Albanis, T.A. (1999) TiO₂-assisted photocatalytic degradation of azo dyes in aqueous solution: kinetic and mechanistic investigations : A review, *Appl. Catal. B: Environ.*, 19: 1–14.